

## **Topology of chemical ordering and influence on optical band gap in ternary Se-In-Bi chalcogenide glasses**

**Mosimanegape Thobega, Stephen T. Sathiaraj, Kelebogile Maabong and Cosmas M. Muiva\***

*Department of Physics, University of Botswana, P/Bag UB-0022, Gaborone, Botswana*

---

### **ABSTRACT**

*Spectrophotometric measurements were performed on flash evaporated amorphous  $Se_{90-x}In_{10}Bi_x$  ( $x= 0, 2, 4, 6, 8, 10$ ) thin films. The complex dielectric constant ( $\epsilon$ ) was determined from  $n$  and  $k$  spectra and was observed to increase with Bi content. The optical band gap ( $E_g^{opt}$ ) values were determined from the experimental data and compared against the theoretical ones obtained from the Shimakawa model which is based on the Random Band Network (RBN) theory. There was close correlation between the  $E_g^{opt}$  values obtained from the two methods. The observed strong dependence of the optical band gap on Bi additive was explained on the basis of topological and chemical bond energy modifications and increased density of localized states in the mobility gap.*

**Keywords:** Se-In-Bi, band gap, Topology, bond energies.

---

### **INTRODUCTION**

Chalcogenide glasses are an important class of materials formed from group VI chalcogen elements; usually S, Se and Te. Much effort has been devoted to their study in the past decade, owing to their interesting optical properties such as wide transmission window from visible up to far infrared (IR), higher values of non-linear refractive indices [1], high absorption coefficient and lower values of phonon energies [2]. These properties provide rich avenues for a wide range of applications such as optical data storage, photovoltaic solar cells, xerography, phase change memory devices, threshold switching and medical applications such as laser surgery and imaging in mammography [1, 3].

The most common applications of chalcogenide glasses are based on their optical properties [4]. Hence, a comprehensive understanding of the electronic band structure, optical and dielectric properties of these materials is of crucial importance [5]. Among the chalcogenide glasses, Se based glass alloys, in both amorphous and polycrystalline forms are very interesting materials which have found numerous applications based on their electrical and optical properties [5]. Applications of pure amorphous Se are limited by its shortcomings such as thermal instability, short lifetime, low sensitivity and low crystallization temperature [6, 7]. However, addition of a second element (e.g *In, Bi, Ge, Sb, Ag, Sn, As, Pb, Zn*) or another chalcogenide (*S, Te*) can enhance mechanical properties, alter structural, optical and electrical properties and reduce ageing. Recently, ternary glassy alloys formed by addition of a third element to a binary system are a subject of considerable technological interest.

Se-In alloys have low glass transition temperatures, low mechanical strength and may deteriorate in properties during long term use. Further, it is believed that the glass forming threshold in Se-In system lies in the vicinity of  $Se_{90}In_{10}$  [8, 9, 10]. This is the critical composition bordering on the rigidity percolation threshold (RPT) where the system changes from floppy to a chemically ordered matrix. It is believed that alloying of these critical Se-In glasses

with Bi can expand the glass forming region, create compositional disorder [11] and open new avenues of application possibilities. To our knowledge, reports on  $\text{Se}_{90-x}\text{In}_{10}\text{Bi}_x$  are very limited. In this work the effect of addition of Bi on the dielectric parameters and optical band gap of  $\text{Se}_{90-x}\text{In}_{10}\text{Bi}_x$  ( $x = 0, 2, 4, 6, 8, 10$ ) films, prepared by flash vacuum evaporation technique is reported. Furthermore, the composition induced trends in the band gap values have been discussed in terms of topological and bond energy parameters of the alloys.

## MATERIALS AND METHODS

Bulk samples of  $\text{Se}_{90-x}\text{In}_{10}\text{Bi}_x$  ( $x = 0, 2, 4, 6, 8, 10$ ) glassy alloys were prepared from high purity (99.999%) elements of Selenium, Indium and Bismuth by the conventional melt quenching technique. Selenium, indium and Bismuth were crushed to powder and equivalent ratios of  $\text{Se}_{90-x}\text{In}_{10}\text{Bi}_x$  ( $x = 0, 2, 4, 6, 8, 10$ ) were weighed into bulk batches of 4 g. The mixture was then put in silica ampoules and sealed under a vacuum pressure of  $10^{-3}$  torr using an oxy-acetylene torch. The sealed ampoules were then put in an Elite Thermal Systems TSH16/50/450-2216 stepping furnace to melt the samples. The furnace temperature was raised to 923 K in steps of about 25 K every 10 minutes and held at this temperature for 8 hours. During the melting process, the ampoules were periodically agitated to thoroughly mix the alloys. At the end of 8 hours the samples were removed and immediately quenched in ice cold water to retain and freeze the amorphous structure. The silica ampoules were then broken to recover the glassy samples which were then powdered ready for evaporation.

Thin films were synthesized by flash evaporation of the powdered bulk samples in a high vacuum chamber. The vacuum chamber featured an Edwards Auto 306 Coating chamber operating at a running base pressure of  $10^{-5}$  torr. The samples were weighed into tantalum boats attached between two electrodes within the chamber. Pre-cleaned glass substrates were then placed directly above the sample boat at a distance of 0.15 m. Then the samples were evaporated by resistance heating onto the glass substrates without any intentional heating of the glass substrates. The transmittance and reflectance of each sample were measured using a CARY 500 UV/VIS/NIR double beam spectrophotometer within the spectral range 300-2500 nm. The film thickness was obtained using a P-15 KLA Tencor stylus surface profiler. A Scanning Electron Microscope (SEM) with Energy Dispersive Spectroscopy (EDS) attachment was used to further analyze the elemental composition of the samples.

### 3. Experimental determination of the optical band gap of $\text{Se}_{90-x}\text{In}_{10}\text{Bi}_x$

The dispersion of refractive index ( $n$ ) was obtained from the envelope method as described by Swanepoel [12]. The fundamental electron excitation spectrum of a film is described by means of frequency ( $\nu$ ) dependence on the complex dielectric constant ( $\epsilon$ ), defined as [13];

$$\epsilon = \epsilon_r(\nu) + \epsilon_i(\nu) \quad (1)$$

where  $\epsilon_r$  and  $\epsilon_i$  are the real and imaginary parts of the dielectric function respectively. These two components are related to refractive index ( $n$ ) and extinction coefficient ( $k$ ) through the expressions;

$$\epsilon_r = n^2 - k^2 \quad (2)$$

$$\epsilon_i = 2nk \quad (3)$$

Fig. 1 shows  $k$  as a function of wavelength. It was observed that  $k$  decreases with increasing wavelength in the region (650-1000) nm and levels out beyond this region.  $k$  is correlated to absorption of photons and is expected to drop drastically after the cut off wavelength and into the region of higher transmittance.

In the region of low absorption where  $k \rightarrow 0$ ,  $\epsilon_r \approx n^2$ .  $\epsilon_r$  controls how radiation is refracted (slowed) while the  $\epsilon_i$  is related to absorption of energy due to dipole dislocation. Figs. 2 and 3 show the dependence of  $\epsilon_r$  and  $\epsilon_i$  on the photon energy ( $h\nu$ ), respectively. It was observed that  $\epsilon_r$  and  $\epsilon_i$  increase with increasing Bi and photon energy. Both  $\epsilon_r$  and  $\epsilon_i$  are proportional to the refractive index. It can be concluded that there was high refraction of radiation within the amorphous thin films at high photon energy. On the other hand, the increase in  $\epsilon_r$  and  $\epsilon_i$  with Bi content may be attributed to the increase in density of defects states in incorporating Bi to the host  $\text{Se}_{90-x}\text{In}_{10}\text{Bi}_x$  [14] and polarizability of the larger Bi atom as compared to Se.

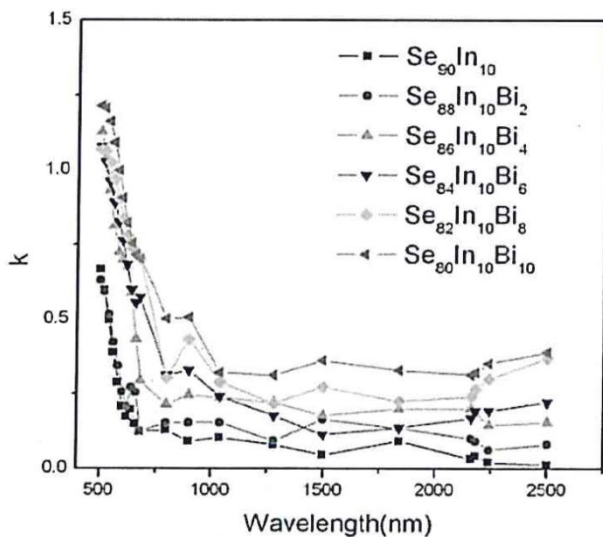


Figure 1: Spectral dependence of extinction coefficient with wavelength

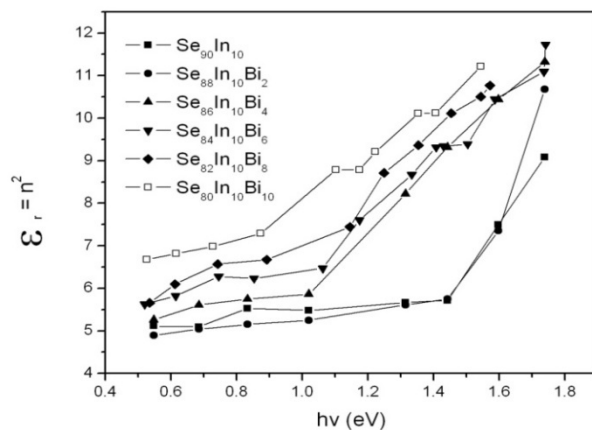


Figure 2: Spectral dependence of  $\epsilon_r$  on  $h\nu$  for  $Se_{90-x}In_{10}Bi_x$  thin films

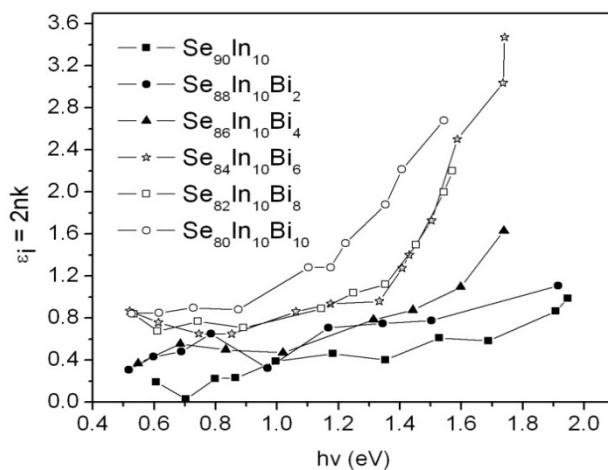


Figure 3: Spectral dependence of  $\epsilon_i$  on  $h\nu$  for  $Se_{90-x}In_{10}Bi_x$  thin films

Fig. 4 shows dependence of  $2nk$  values on photon energies and the plots reveal that the amount of light absorbed or scattered is a function of wavelength and increases rapidly for energies greater than the absorption edge. As mentioned earlier,  $n$  and  $k$  are related to the amount of light absorbed or/and scattered.

According to Abdel-Aziz [15], the optical band gap ( $E_g^{opt}$ ) can be found from the relation;

$$hv(2nk)^{1/2} = (hv - E_g^{opt}) \quad (4)$$

where ( $2nk = \varepsilon_i$ ) is the imaginary part of the dielectric constant. This is done by plotting  $hv(2nk)^{1/2}$  against photon energy ( $hv$ ) and extrapolating the linearly dependent parts to regions where  $hv(2nk)^{1/2} = 0$ . Fig. 4 below shows plots of  $hv(2nk)^{1/2}$  against  $hv$  and the obtained values  $E_g^{opt}$  are listed in Table 1. The observed values were within the range of 0.93-1.54 eV and were observed to decrease with increasing Bi content.

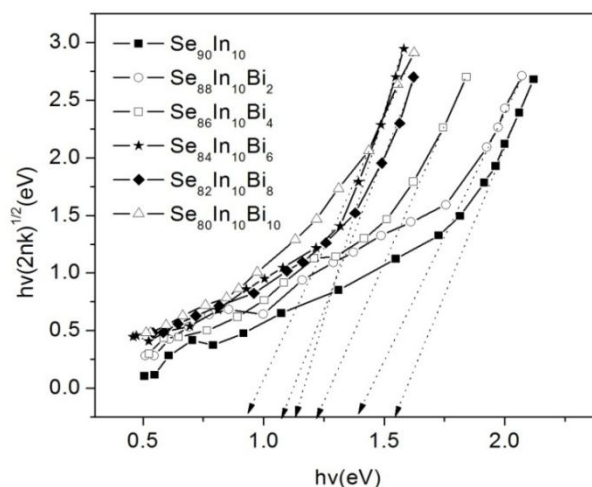


Figure 4: Plot of  $hv(2nk)^{1/2}$  against photon energy ( $hv$ ) for  $Se_{90-x}In_{10}Bi_x$  amorphous films

Table1: Experimental and theoretical values of the band gap.

Alloy	Experimental $E_g^{opt}$ (eV)	Theoretical $E_{gt}^{opt}$ (eV)
$Se_{90}In_{10}$	1.54	1.52
$Se_{88}In_{10}Bi_2$	1.39	1.38
$Se_{86}In_{10}Bi_4$	1.22	1.25
$Se_{84}In_{10}Bi_6$	1.13	1.15
$Se_{82}In_{10}Bi_8$	1.07	1.06
$Se_{80}In_{10}Bi_{10}$	0.93	0.98

#### 4. Theoretical determination of band gap ( $E_{gt}^{opt}$ )

The optical band gap of amorphous thin films depends on composition of the alloy. Shimakawa [16] has introduced a theoretical model for determining optical band gap based on the random band network [RBN], and has the form [16];

$$E_{g(AB)} = Y(E_{gA}) + (1 - Y)E_{gB} \quad (5)$$

where  $Y$  and  $(1-Y)$  are the volume fractions of elements A and B and  $E_{gA}$  and  $E_{gB}$  are the optical band gaps of elements A and B respectively. The obtained values of the theoretical band gap,  $E_{gt}^{opt}$  are also listed in Table 1. It is clear that the optical band gap values obtained from the two methods are in good agreement. The slight difference may be due to different approximations used for each method. Agreement of the two methods indicates that the observed compositional trends in the band gap values can be explained by topological and bond energy indicators.

It seems no single model can be used to explain the compositional trends of  $E_g^{opt}$  in chalcogenide glasses. The direction of certain properties in chalcogenide glasses can be visualized in terms of mechanical and chemical forces

which affect the structure of the system [17]. These include; the effective average coordination number  $\langle r \rangle$ , the number of constraints arising from bond bending ( $N_b$ ) and bond stretching ( $N_s$ ) given by [18];

$$\langle r \rangle = \frac{\alpha r_A + \beta r_B + \gamma r_C}{\alpha + \beta + \gamma} \quad (6)$$

where  $\alpha$ ,  $\beta$  and  $\gamma$  are the atomic percentages of each of the species A, B, and C, respectively.  $r_A$  is simply the coordination number of species A and is referred to as the number of nearest neighbor atoms.  $r = 2, 5$  and  $3$  for Se, In and Bi respectively. The total number of constraints arising from bond bending and bond stretching are calculated from  $\langle r \rangle$  using the expression [19];

$$N_c = N_b + N_s = (5 \langle r \rangle / 2) - 3 \quad (7)$$

where the total number of constrains ( $N_c$ ) is the sum of both angular ( $N_b = 2 \langle r \rangle - 3$ ) and radial ( $N_s = \langle r \rangle / 2$ ) constrains [20]. The calculated values of  $\langle r \rangle$ ,  $N_s$ ,  $N_b$  and  $N_c$  are recorded in Table 2. It is observed that  $N_c$  increase with Bi from a minimum of 2.75 for  $\text{Se}_{90}\text{In}_{10}$  ( $x = 0$  at%) to 3.00 for  $\text{Se}_{80}\text{In}_{10}\text{Bi}_{10}$  ( $x = 10$  at%). In line with topological predictions, at this latter composition,  $N_c$  equals to the number of degrees of freedom. In most chalcogenide glassy systems, the so-called  $8-N$  rule, where  $N$  is the number of electrons in outer shell is obeyed. According to this rule, if the number of constrains ( $N_c$ ) exhaust the number of degrees of freedom; i.e  $N_c > 3$  the glass becomes rigid. In the range studied, the number of constrains do not exhaust the number of degrees of freedom except in  $\text{Se}_{80}\text{In}_{10}\text{Bi}_{10}$  which lies in the critical composition where  $N_c = 3$ , i.e where the floppy modes are exhausted and the system moves towards the intermediate region.

**Table 2: Average coordination number ( $\langle r \rangle$ ), deviation from stoichiometry (R), electronegativity ( $\chi$ ), number of bond stretching ( $N_s$ ), bond bending ( $N_b$ ) and total number of constrains ( $N_c$ )**

Alloy	$\langle r \rangle$	R	$\chi$	$N_s$	$N_b$	$N_c$
$\text{Se}_{90}\text{In}_{10}$	2.30	4.50	2.47	1.15	1.60	2.75
$\text{Se}_{88}\text{In}_{10}\text{Bi}_2$	2.32	3.83	2.46	1.16	1.64	2.80
$\text{Se}_{86}\text{In}_{10}\text{Bi}_4$	2.34	3.31	2.45	1.17	1.68	2.85
$\text{Se}_{84}\text{In}_{10}\text{Bi}_6$	2.36	2.90	2.44	1.18	1.72	2.90
$\text{Se}_{82}\text{In}_{10}\text{Bi}_8$	2.38	2.56	2.43	1.19	1.76	2.95
$\text{Se}_{80}\text{In}_{10}\text{Bi}_{10}$	2.40	2.29	2.42	1.20	1.80	3.00

The deviation from stoichiometry R was calculated according Tichy and Ticha [21] and listed in Table 2. According to this group,  $R > 1$  for chalcogen rich,  $R = 1$  at stoichiometric composition and  $R < 1$  for chalcogen deficient samples. In the entire range studied  $R > 1$  depicting chalcogen rich glasses.

Optical band gap has been identified as a bond-sensitive property [22] that depends on compactness, density and network connectivity (rigidity). These factors also show composition dependence. To this end, the authors thought it was worth to calculate the overall cohesive energy (mean stabilization energy)  $\langle E \rangle$  for each composition and observe trends in  $\langle E \rangle$  and band gap behavior to see if there are any peculiar similarities. According to topological theories, bond energies of alloys are purely additive. Therefore, the overall cohesive energy is the geometric sum of energies of the individual bonds present in the glass structure based on their relative proportions. The overall mean cohesive energy is expressed as [21];

$$\langle E \rangle = E_c + E_{rm} \quad (8)$$

Where  $E_c$  is the contribution towards overall bond energy arising from strong heteropolar bonds and  $E_{rm}$  is the contribution arising from the remaining weaker bonds that remain after the strong bonds have been maximized [23].  $\langle E \rangle$  is a function of  $\langle r \rangle$ , type of bonds and bond energy [24]. The observed values of  $\langle E \rangle$  are listed in Table 3 and their decrease with addition of Bi implies lower binding energy and may have contributed to the monotonous drop in  $E_g^{\text{opt}}$ .

Table 3: Atomization energy ( $H_s$ ), average single bond energy ( $H_s/\langle r \rangle$ ) and overall mean bond energy ( $\langle E \rangle$ )

Alloy	$H_s$ (Kj/mol)	$H_s/\langle r \rangle$ (Kj/mol)	$\langle E \rangle$ (Kj/mol)
Se <sub>90</sub> In <sub>10</sub>	210.44	91.50	76.89
Se <sub>88</sub> In <sub>10</sub> Bi <sub>2</sub>	210.45	90.71	75.11
Se <sub>86</sub> In <sub>10</sub> Bi <sub>4</sub>	210.46	89.94	73.40
Se <sub>84</sub> In <sub>10</sub> Bi <sub>6</sub>	210.47	89.18	71.76
Se <sub>82</sub> In <sub>10</sub> Bi <sub>8</sub>	210.48	88.44	70.20
Se <sub>80</sub> In <sub>10</sub> Bi <sub>10</sub>	210.49	87.71	68.69

The chemical ordered covalent network model (COCN) [23] was used to predict the distribution of bonds in the present system. This model is based on the premise that atoms have more tendencies to bond with dissimilar atoms than with themselves. This implies that heteronuclear bonds are more preferable than homonuclear bonds. During these preferential assembling of bonds, the bonds are formed on the sequence of bond energies with the strongest bonds formed first. The bonds possibilities in this system are, Se-Se, In-In, Bi-Bi, Se-In, Se-Bi and In-Bi. The bond energies for heterogeneous compositions  $D_{A-B}$  were calculated from the homonuclear ( $D_{A-A}$  and  $D_{B-B}$ ) bond energies based on the Pauling's theory [25];

$$D_{A-B} = (D_{A-A} * D_{B-B})^{1/2} + 30(\chi_A - \chi_B)^2 \quad (9)$$

Where  $D_{A-A}$  and  $D_{B-B}$  are the bond energies of homonuclear bonds for elements A and B, respectively and  $\chi_A$  and  $\chi_B$  are the corresponding electronegativities. The bond energies of various bonds involved in the system are given by  $D_{Se-Se} = 184.1$  Kj/mol,  $D_{In-In} = 101.25$  Kj/mol and  $D_{Bi-Bi} = 104.6$  Kj/mol and the corresponding electronegativities are  $\chi_{Se} = 2.55$ ,  $\chi_{In} = 1.78$  and  $\chi_{Bi} = 2.05$  [25, 26]. The calculated Se-In heteropolar bond energy is 227.22 Kj/mol and that of Se-Bi is 170.12 Kj/mol. In addition, the geometric mean electronegativity ( $\chi$ ) of each composition was calculated and the values entered in Table 2. The bond energy of Se-In is highest, therefore Se-In bonds will be formed first until all the indium is exhausted followed by Se-Bi. Considering that the deviation from stoichiometry  $R > 1$  (Table 2) for the entire range of composition, then only heteronuclear and Se-Se bonds will be existing and no metallic bonds (In-In or In-Bi) are expected. This therefore implies that since the amount of *In* is fixed and Se-In bonds are favored, addition of Bi into the system will favor replacement of stronger Se-Se bonds by weaker Se-Bi bonds with bond energy adjustment from 184.1 Kj/mol to 170.12 Kj/mol respectively. This therefore reduces the overall cohesiveness of the system.

According to Pauling [27], for a binary semiconductor of the form  $A_\alpha B_\beta$ , the heat of atomization  $H_{S(A-B)}$  at standard temperature and pressure is the sum of the formation heats ( $\Delta H$ ) and the average heats of atomization ( $H_s$ ) that correspond to the average non polar bond energy of the ternary;

$$H_{S(A-B)} = \Delta H + 1/2(H_{S,A} + H_{S,B}) \quad (10)$$

Assuming that  $\alpha$ ,  $\beta$  and  $\gamma$  are the corresponding atomic combination for the species A, B and C respectively,  $H_s$  can be written as [28];

$$H_s = (\alpha H_{S,A} + \beta H_{S,B} + \gamma H_{S,C}) / (\alpha + \beta + \gamma) \quad (11)$$

Where  $H_{S,A}$ ,  $H_{S,B}$  and  $H_{S,C}$  are the heat of atomization of atoms A, B and C, respectively. The assumptions referred to herein have been described elsewhere [20, 29, 30]. Furthermore the quotient of average heats of atomization and mean coordination number, denoted as the average single bond energy ( $H_s/\langle r \rangle$ ) was calculated and values entered in Table 3. The linearity of these topological and bond energy constants with Bi content was recently and exhaustively reported by Gupta *et al* [31] in Ge-Se-Bi system.

The relationship between the optical energy gap and binding energy indicators was discussed by Aigrain *et al* [32] who proposed that for certain type of semiconductors of the diamond and Zinc-blende structure there exists a linear correlation that can be expressed by;  $E = a(E_s - b)$ , where a and b are constants.  $E_s$  is a parameter that is related to the cohesive energy of the system such as  $H_s/\langle Z \rangle$ . Therefore, the monotonous decrease of  $E_g^{opt}$  with addition of Bi may be correlated to decrease in  $H_s/\langle Z \rangle$  (Table 3) [33]. Similar effects due to Bi additive were reported by Sharma *et al* [34] in  $Ge_{20}Se_{80-x}Bi_x$ . It has been pointed out that this bond approach neglects defects such as dangling bonds and other valence defects which generate localized defect states in the mobility gap which decreases  $E_g^{opt}$ . These defects

and contribution of the weaker Van der Waals forces towards bond energies [35] provide weaker links than regular covalent bonds and provide further stabilization of the structure [30].

### CONCLUSION

The Shimakawa theoretical model and experimental techniques were used to obtain the optical band gap ( $E_g^{opt}$ ) in flash evaporated amorphous  $Se_{90-x}In_{10}Bi_x$  ( $x = 0, 2, 4, 6, 8, 10$ ) thin films. The closeness of the values obtained from the two methods implied that the band gap could be explained on the basis of topology. There was a monotonous drop in  $E_g^{opt}$  values with increasing Bi content which was attributed to changes in topology, bond energies and increased density of localized states in the energy gap.

### Acknowledgements

The authors acknowledge the University of Botswana through research grant R907 for supporting this work.

### REFERENCES

- [1] A. Zakery, S.R Elliot, *J. Non-Cryst. Sol.*, **2003**, 330, 1
- [2] N. Mehta, *J. Sci. Ind. Res.*, **2006**, 65, 777
- [3] D.W. Piraino, W.J. Davros, M. Lieber, B.J. Richmond, J.R Schils, M.P. Recht, P.N. Grooff, G.H. Belhobek, *American Journal Roentgenology*, **1999**, 172, 177
- [4] M. Kapoor, N. Thakur, *Turk J. Phys.*, **2011**, 35, 1
- [5] S. Srivastava, N. Mehta, R. S. Tiwari, R. K. Shukla, A. Kumar, *J. Optoelectron. Adv. Mater.*, **2011**, 13 (1), 13
- [6] M.F. Kotkata, Sh. A. Mansour, *J. Therm. Anal. Calorim.*, **2011**, 103, 555
- [7] N. Mehta, D. Kumar, S. Kumar, A. Kumar, *Chalcogenide Letters*, **2005**, 2 (10), 103
- [8] M.F. Kolkata, S.A. Mansour, *J. Appl. Phys. A: Mater. Sci. Proc.*, **2012**, 107(4), 1003
- [9] M.M.A. Imran, O. A. Lafi, *Mater. Chem. and Phys.*, **2011**, 129 1201,
- [10] K. Singh, D. Patidar, N.S. Saxena, *J. Phys. Chem. Solids*, **2005**, 66, 946
- [11] A. Khan, M. Zulfequar, M. Husain, *Solid State Communication*, **2002**, 123, 463
- [12] R. Swanepoel, *J. Phys. E: Sci. Instrum.*, **1984**, 17, 896
- [13] T.S Sathiaraj, *Transactions of the Material Society of Japan*, **1998**, 29 (4), 1455
- [14] M. A. Majeed Khan, Sushil Kumar, M. Husain, M. Zulfequar, *Journal of Non-Oxide Glasses*, **2009**, 1(1), 71
- [15] M.M. Abdel-Aziz, E.G. El-Metwally, M. Fadel, H.H. Labib, M.A. Afifi, *Thin Solid Films*, **2001**, 386, 99
- [16] K. Shimakawa, *J. Non-Cryst. Sol.*, **1981**, 43, 229
- [17] A.F. Loffe, A.R. Regel, *Progress in Semiconductors*, **1960**, 4, 239
- [18] J.C. Phillips, *J. Non-Cryst. Sol.*, **1979**, 34, 153
- [19] M. Micoulaut, J.C. Phillips, *Phys. Rev. B*, **2003**, 67, 104204
- [20] A. Kumar, P.B. Barman, R. Sharma, *Advances in Applied Science Research*, **2010**, 1(2), 47
- [21] L. Tichy, H. Ticha, *J. Non-Cryst. Sol.*, **1995**, 189, 141
- [22] A.K. Pattanaik, A. Srinivasan, *J. Optoelectron. Adv. Mater*, **2003**, 5 1161
- [23] W.H. Zachariasen, *J. Am. Chem. Soc.*, **1932**, 54, 3841
- [24] D. Singh, S. Kumar, R. Thangaraj, *Advances in Applied Science Research*, **2011**, 2(3), 20
- [25] L Pauling, *The Nature of the Chemical Bond* (3rd Edition), Cornell University Press, Ithaca, NY, **1960**
- [26] S.S. Fouad, *Physica B*, **1999**, 270, 360
- [27] L. Pauling, *J. Phys. Chem.*, **1954**, 58, 662
- [28] I. Sharma, S.K. Tripathi, P.B. Barman, *Philos. Mag.*, **2008**, 88, 3081
- [29] S. Tiwari, A. K. Saxena and D. Saxena, *Advances in Applied Science Research*, **2011**, 2(5), 77
- [30] A.A. Othman, K.A. Aly, A.M. Abousehly, *Thin Solid Films*, **2007**, 515, 3507
- [31] S. Gupta, M. Saxena, S. Chawla, *Advances in Applied Science Research*, **2013**, 4(3), 244
- [32] C. Benoit, P. Aigrain, M. Balkanski, *Selected Constants Relative to Semiconductors*, Pergamon Press, New York, **1961**
- [33] N. El-Kabany, *Vacuum*, **2010**, 85, 5
- [34] P. Sharma, M. Vashistha, I. P. Jain, *J. Optoelectron. Adv. Mater*, **2005**, 7(6), 2963
- [35] G. Saffarini, J.M. Saiter, H. Schmitt, *Optical Materials*, **2007**, 29, 1143